

Modeling of Symmetrical Squirrel Cage Induction Machine with MatLab Simulink

Marcus Svoboda*, Lucian Tutelea*, Gheorghe Madescu**, Marius Biriescu*, Martian Mot**

* University POLITEHNICA Timisoara/Electrical Engineering, Timisoara, Romania

** Romanian Academy – Branch Timișoara

marcus.svoboda@upt.ro; lucian.tutelea@upt.ro; gmadescu@d109lin.upt.ro; marius.biriescu@upt.ro; martian.mot@upt.ro

Abstract — The aim of this paper is to develop a MatLab Simulink dynamical model based on mathematical dq model of a squirrel cage induction machine, for having direct access to the rotor bars current. The simulation was performed with actual parameters data of a standard 4 kW, four poles, induction motor with cage rotor. This paper presents this model and some results on full load and starting conditions.

I. INTRODUCTION

The induction motor belongs to the class of electric rotating machines. The important property of all electrical machines is the principle of reversibility: electrical machine can transform mechanical energy into electrical energy and vice versa [1]. The squirrel-cage rotor induction motor is the most widely used AC motor because of its simple construction, low cost, reliability in operation and easy maintenance, no one can deny the important role of asynchronous motor in industry applications [2], [3]. An induction motor, therefore, does not require mechanical commutation, separate-excitation or self-excitation for all or part of the energy transferred from stator to rotor, as in universal, DC and synchronous motors.

When an electrical motor is viewed as a mathematical system, with inputs and outputs, it can be analyzed and described in multiple ways, considering different reference frames and state-space variables. Simulink induction machine models are available in the literature, but they appear to be black-boxes with no internal details. Some of them [4], [5] recommend using S-functions, which are software source codes for Simulink blocks. This technique does not fully utilize the power and ease of Simulink because S-function programming knowledge is required to access the model variables.

In an induction motor, the 3-phase stator windings are designed to produce sinusoidal distributed mmf (magnetomotiv force) in space along the air gap periphery. Assuming uniform air gap and neglecting the effects of slot harmonics, distribution of magnetic flux will also be sinusoidal. It is also assumed that the neutral connection of the machine is open so that phase voltages, currents and flux linkages are always balanced and there is no *zero phase sequence* component in the system. The cage contains conductive bars of aluminum or copper connected both ends by shorting rings outside of a magnetic iron core.

II. MATHEMATICAL MODEL FOR SQUIRREL CAGE INDUCTION MOTOR

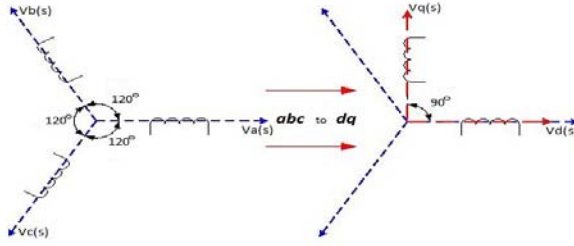
Some authors [6], [7], [8] used for modeling the dq model for squirrel cage induction machine the coupled magnetic circuit theory, which consist in describing the machine as a set of multiple coupled circuits defined by inductance matrices (self and mutual, in correlation with rotor position) [9]. This approach, for a machine having n rotor bars result a model with $n+3$ nonlinear simultaneous differential equation, plus the mechanical equation. This method has a big drawback consist in huge computation time and power.

Applying the Park's transformation to the abc model of squirrel cage induction motor, is obtained the dq model of the machine [10].

In Fig. 1 is presented the dq model transformation.

This transformation eliminates mutual magnetic coupling between the phases and therefore makes the magnetic flux linkage of one winding independent of the current of another winding. This model is given by the follow equations (for a_0, a_1, a_2 see Annex 1):

$$\begin{aligned}
 \frac{d\psi_{qs}}{dt} &= V_{qs} - R_s * I_{qs} - \omega * \psi_{ds} \\
 \frac{d\psi_{ds}}{dt} &= V_{ds} - R_s * I_{ds} - \omega * \psi_{qs} \\
 \frac{d\psi_{qr}}{dt} &= -R_r * I_{qr} - (\omega - \omega_r) * \psi_{dr} \\
 \frac{d\psi_{dr}}{dt} &= -R_r * I_{dr} - (\omega - \omega_r) * \psi_{qr} \\
 I_{qs} &= \psi_{qs} * a_1 - \psi_{qr} * a_2 \\
 I_{ds} &= \psi_{ds} * a_1 - \psi_{dr} * a_2 \\
 \psi_{qr} &= L_r * I_{qr} + L_m * I_{qs} \\
 \psi_{dr} &= L_r * I_{dr} + L_m * I_{ds} \\
 \psi_{qs} &= L_s * I_{qs} + L_m * I_{qr} \\
 \psi_{ds} &= L_s * I_{ds} + L_m * I_{dr} \\
 L_s &= L_{1s} + L_{ms} \\
 L_r &= L_{1r} + L_{ms} \\
 \omega_r &= \omega * \frac{p}{2}
 \end{aligned} \tag{1}$$



From the system (1), equations model for q-axis are:

$$R_s * I_{qs} + \left(L_s - \frac{L_{ms}^2}{L_r} \right) * \frac{dI_{qs}}{dt} = V_{qs} - \frac{L_{ms}}{L_r} * \frac{d\psi_{qr}}{dt} \quad (2)$$

$$\frac{L_r}{R_r} * \frac{d\psi_{qr}}{dt} + \psi_{qr} = I_{qs} * L_{ms} + \frac{L_r}{R_r} * \left(\omega * \frac{P}{2} \right) * \psi_{dr} \quad (3)$$

Equations model for d-axis:

$$R_s * I_{ds} + \left(L_s - \frac{L_{ms}^2}{L_r} \right) * \frac{dI_{ds}}{dt} = V_{ds} - \frac{L_{ms}}{L_r} * \frac{d\psi_{dr}}{dt} \quad (4)$$

$$\frac{L_r}{R_r} * \frac{d\psi_{dr}}{dt} + \psi_{dr} = I_{ds} * L_{ms} + \frac{L_r}{R_r} * \left(\omega * \frac{P}{2} \right) * \psi_{qr} \quad (5)$$

Torque equations:

$$T_e = \frac{L_m}{2} * \frac{1}{\frac{k_r}{k_s}} * \sqrt{\frac{N_r}{3}}, \quad (6)$$

where: ψ_{ds} , ψ_{qs} - stator fluxes; ψ_{dr} , ψ_{qr} - rotor fluxes; V_{qs} , V_{ds} - d, q stator voltages components; R_s , R_r - stator and rotor resistance; I_{ds} , I_{qs} - d, q stator currents components; I_{dr} , I_{qr} - d, q rotor currents components; ω - speed; ω_e - nominal angular speed; P- the pole number; L_s , L_r - stator and rotor inductances; L_{1s} , L_{1r} - stator and rotor leakage inductance; L_{ms} - mutual inductance; T_e - electromagnetic torque; k_r , k_s - rotor respectively stator coefficients; N_r - number of rotor bars.

Usually, in analysis and design of 3-phase induction motors, the “per-phase equivalent circuit” has been widely used. This equivalent model for one phase of squirrel cage induction machine is shown in Fig. 2.

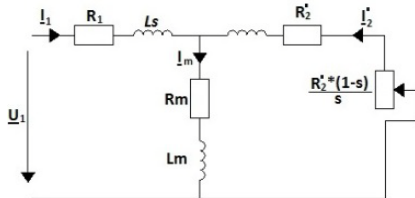


Figure 2. Per phase circuit model of three-phase induction motor

In Fig. 3 and Fig. 4 are presented the actual cage (bars and end-rings) of a machine and the equivalent rotor cage (resistances and inductances) used for modeling.

Rotor flux has two components: self-rotor flux and mutual stator-rotor flux, according to equation:

$$\psi_{rr} = L_{rr} * I_r + L_{rs} * I_s \quad (7)$$

where: L_{rr} –self rotor inductance, is a constant matrix; L_{rs} – mutual stator and rotor inductances matrix, see (8).

$$L_{rr} = \begin{bmatrix} L_{kk} + L_0 & L_{ki} - L_b & L_{ki} & \dots & L_{ki} - L_b & -L_e \\ L_{ki} - L_b & L_{kk} + L_0 & L_{ki} - L_b & \dots & L_{ki} & -L_e \\ \vdots & \vdots & \vdots & \ddots & \vdots & \vdots \\ L_{ki} - L_b & L_{ki} & L_{ki} & \dots & L_{kk} + L_0 & -L_e \\ -L_e & L_e & -L_e & \dots & -L_e & N_r * L_e \end{bmatrix}$$

where $L_0 = 2 * (L_e + L_b)$ – is an auxiliary variable.

$$L_{ki} = -\frac{\mu_0 * l_r}{g} * \alpha_r^2, \text{ with } k \neq 1 \quad (8)$$

$$L_{kk} = \frac{\mu_0 * l_r}{g} * \alpha_r * \left(1 - \frac{\alpha_r}{2 * \pi i} \right) \quad (9)$$

$$L_{sr} = L_{rs}^T = \begin{bmatrix} L_a & L_b & L_c \\ \vdots & \ddots & \vdots \\ L_{a * N_r} & L_{b * N_r} & L_{c * N_r} \end{bmatrix}^T \quad (10)$$

For α_r , L_{ai} , L_{bi} , L_{ci} see Annex 1.

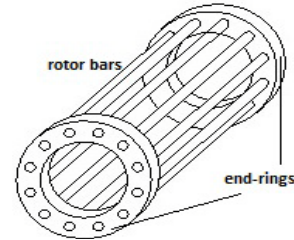


Figure 3. Actual cage (bars and end-rings)

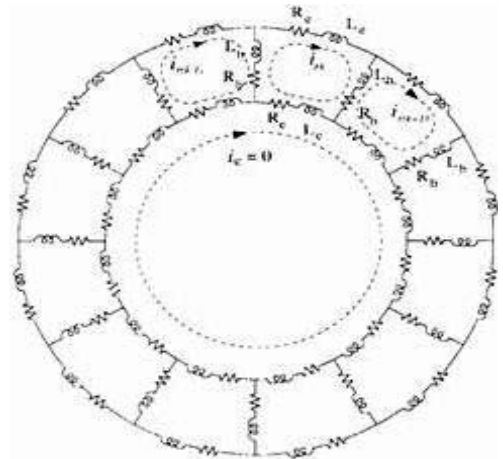


Figure 4. Equivalent model for the rotor cage

III. SIMULATION SCHEME FOR SIMETRICAL SQUIRREL CAGE INDUCTION MACHINE

The proposed simulation scheme was performed in MatLab Simulink, R2012a. The initialization of parameters of the machine (see Annex 2) is made in a matlab file. This scheme is presented in Fig. 5. We can observe the specific blocks for voltage and current transformation, leakage block, speed block, torque block, and rotor currents calculation block.

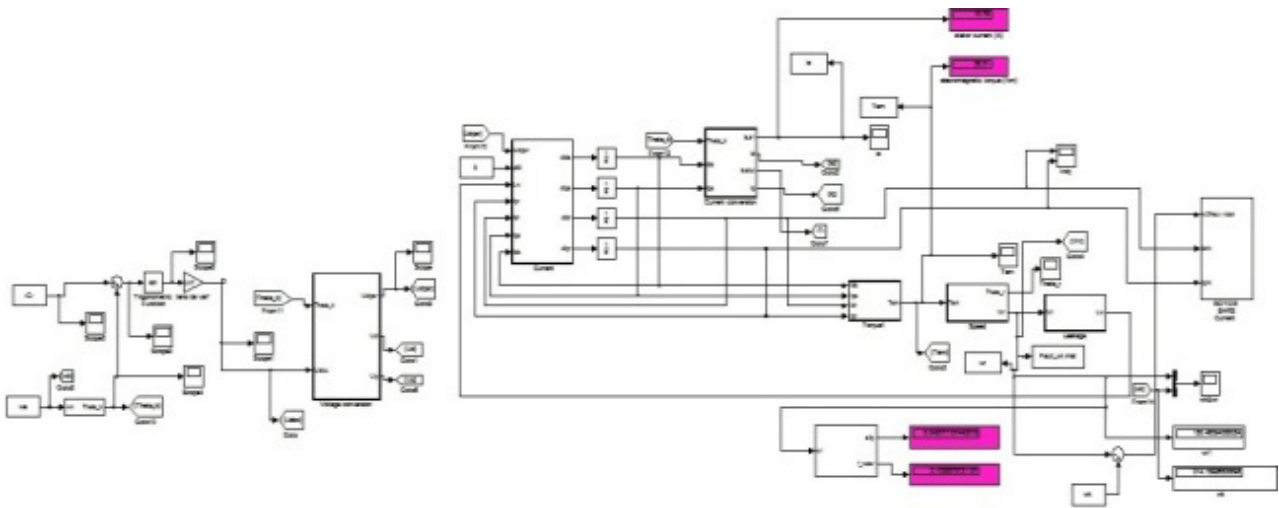


Figure 5. Simulink scheme for squirrel cage induction machine.

All the simulation blocks presented in scheme are created according to equations mentioned above.

Inside the rotor bars current block is implemented the calculus for every current bar, and some detailed are in Fig. 6.

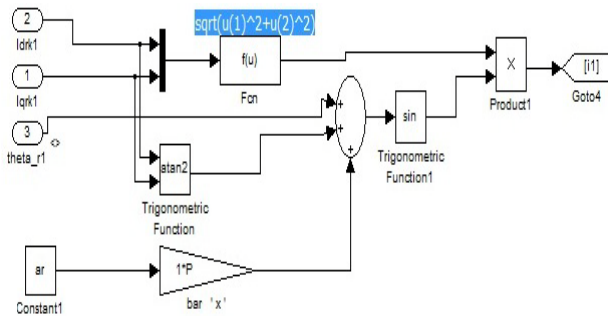


Figure 6. Inside on bar current calculus

In the leakage block is implemented the calculations of proper and mutual inductances of the machine, and, together with the current conversion blocks gives the stator and rotor flux.

IV. SIMULATION RESULTS

The simulations results, for a symmetrical squirrel cage induction machine in direct-quadrature-zero (*dq0*) transformation are presented below. The implemented block scheme can operates in generator, as well as motor mode (depends upon the sign of load torque). The results are focused only for motor operation mode. To be sure that the proposed scheme are work correctly, we simulate a full load start and a short circuit. According to Annex 2, the rated torque of the motor used in simulation is 28 [Nm]. For simulated the short-circuit conditions, the moment of inertia of the machine was artificial increased with 10^6 times.

In Fig. 7 is simulated stator current at starting with full load condition. The frequency is 50 Hz.

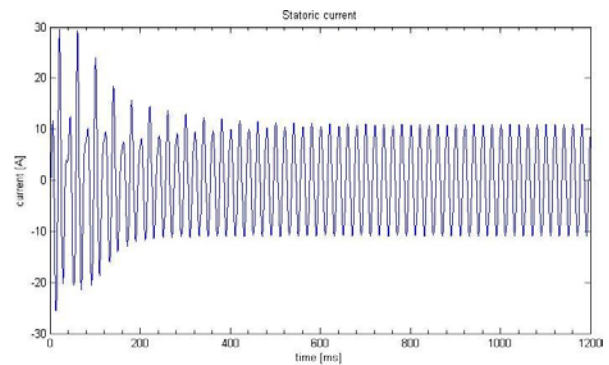


Figure 7. Stator current in transient conditions at starting

Fig. 8 presents the load torque. We can observe the torque, after transient regime is very accurate, according to the imposed value (28 Nm).

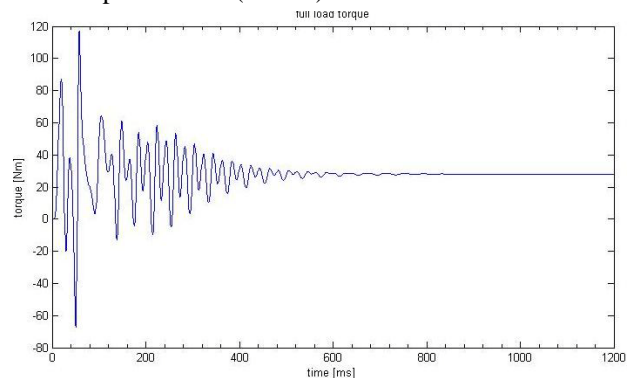


Figure 8. The dynamic torque at start with full load

The rotor bars frequency current and slip are calculated with following equations [11]:

$$f_r = s * f; \quad s = \frac{\omega_n - \omega_r}{\omega_n}, \quad (11)$$

where: ω_n is the synchronous speed; ω_r is the rotor speed; f_r is the frequency of rotor bar currents and f is the frequency of stator current.

Equation (11) was implemented in Simulink blocks, and is presented in Fig. 9. From this figure we can observe the value of rotor current frequency is much lower than stator feed frequency (slip: $s=4.2\%$, $f_r=2.1038$ Hz).

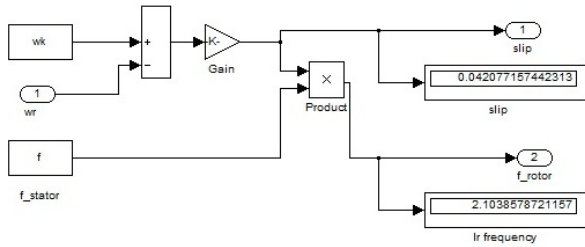


Figure 9. Slip and rotor frequency at full load

The squirrel cage of the simulated motor has 28 bars, and the space distribution of bars currents is represented in Fig. 10. From this figure we can observe the symmetry of the bar currents on the motor poles.

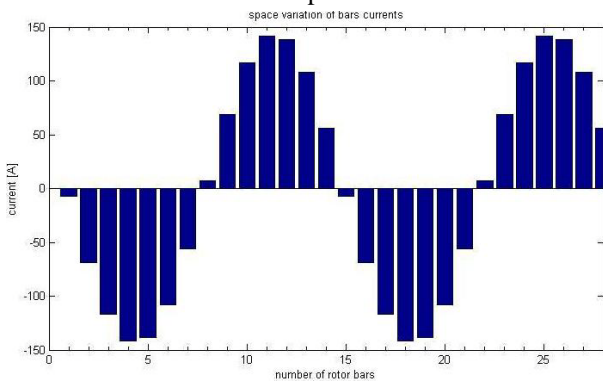


Figure 10. Space distribution of bars currents at full load

In Fig. 11 is presented variation in time for the current in rotor bar No. 5.

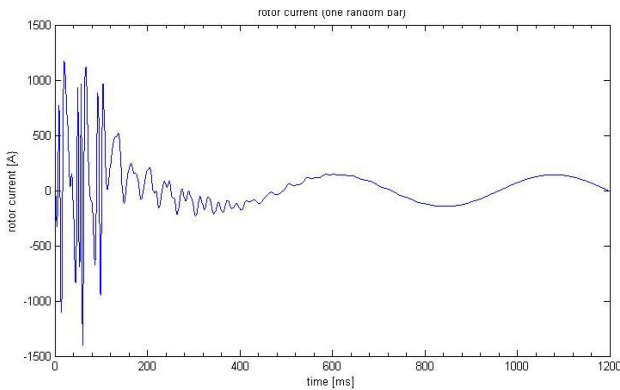


Figure 11. Time variation for current in rotor bar No.5 at full load

For short-circuit simulation, in Fig. 12 is presented the slip and rotor current frequency, in Fig. 13 is presented the space variation of rotor bars current and in Fig. 14 is presented the time variation of rotor bar current in bar No. 5.

From short-circuit simulation (Fig. 12 to 14) we can observe the slip is $s=0.99$, which means the rotor doesn't move ($\omega_r = 0$ [rpm]), in consequence, the rotor current frequency is equal with the stator feed frequency, is 50 [Hz], also the value of the rotor current is increased, compared to full load (see fig. 10, 13) with almost 5 time.

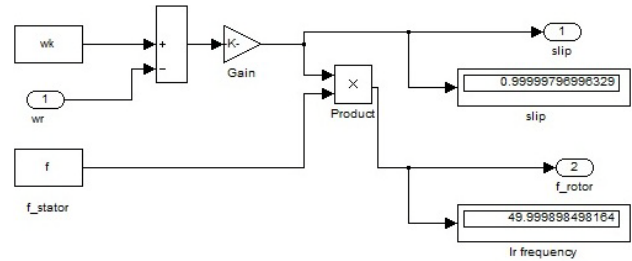


Figure 12. Slip and rotor frequency at short-circuit.

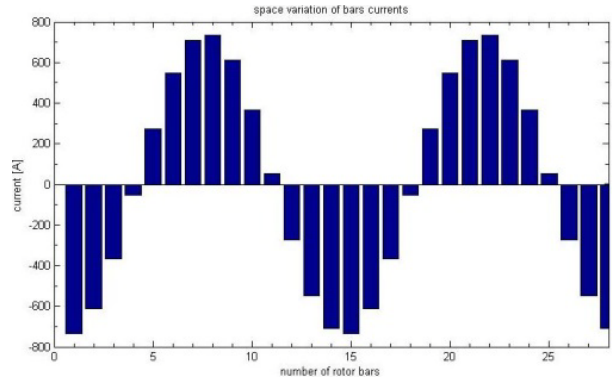


Figure 13. Space distribution of bars currents at short-circuit

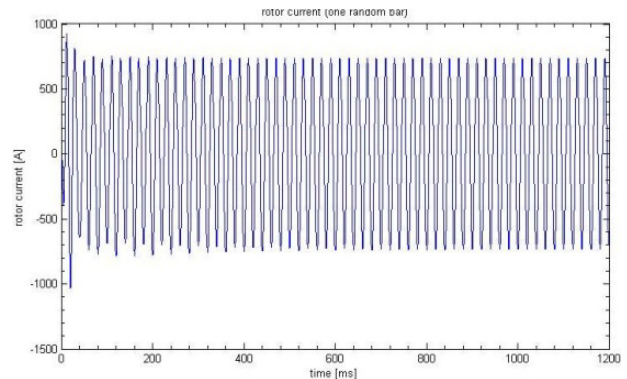


Figure 14. Time variation for current in one rotor bar at short-circuit

V. CONCLUSIONS

A mathematical model of symmetrical squirrel cage induction machine is presented in this paper. The model was transformed in a MatLab Simulink scheme. The model was tested with actual data of a standard 4 kW, 1500 rpm induction motor, in different dynamical conditions. The model was created and adjusted to have access to rotor bars current because this research will be continued to directly measures the bar currents of an experimental prototype and so to validate the model. In such a form, this model is suitable for analyses both dynamical and steady-state behavior of induction machines or diagnosis purposes.

ANNEX 1

$$a_0 = L_s * L_r - L_m^2 ; a_1 = \frac{L_r}{a_0} ; a_2 = \frac{L_m}{a_0} ;$$

$$\alpha_r = \frac{2 * \pi}{N_r} ;$$

$$L_{ai} = L_m * \cos \left[\theta_r + (i - 1) * \alpha_r + \frac{\alpha_r}{2} \right].$$

Respectively L_{bi} and L_{ci} have the same expression, only diphase with 120^0 .

ANNEX 2

INDUCTION MOTOR MAIN PARAMETERS – 4 KW, 1500 RPM

Parameter	Value	Unit
Rated voltage	380 Y	V
Feed frequency	50	Hz
Number of poles	4	-
Stator resistance	1.2	Ω
Bar resistance	90×10^{-6}	Ω
Short-circuit ring resistance	0.82×10^{-6}	Ω
Stator leakage inductance	0.008	H
Bar inductivity	0.438×10^{-6}	H
Short-circuit ring inductance	0.00076×10^{-6}	H
Number of rotor bars	28	-
Number of stator coil	156	-
Equivalent air gap	0.55×10^{-3}	m
Active length of rotor	165×10^{-3}	m
Air gap mean radius	50×10^{-3}	m
Moment of inertia	0.0015	$\text{Kg} \cdot \text{m}^2$
Electromagnetic torque	28	Nm

REFERENCES

- [1] S. A. Nassar, "Electromagnetic energy conversion in nm-winding double cylindrical structures in the presence of space harmonics", *IEEE Trans. On Power, Apparatus and systems*, Vol. 87, pp. 1099-1106, Apr. 1968.
- [2] S., Muşuroi, N., V., Olărescu, D., Vătău, C., Şorândaru, "Equivalent parameters of induction machines windings in permanent regime. Theoretical and experimental determination", *Proceedings of the 9th International Conference on POWER SYSTEMS (PS '09)*, Budapest Tech, Hungary, 3-5 Sept., pp. 55-62, 2009.
- [3] I., Boldea, S. A. Nassar *The induction Machine Handbook – Second edition*, CRC Press, 2009, pp.1-14.
- [4] V., Horcic, "Rotor Faults of the Induction Motors", Mezinárodní konference Technical Computing Prague 2011.
- [5] S. Wade, M. W. Duningam B. W. Williams, "Modeling and simulation of induction machine vector control with rotor resistance identification", *IEEE Trans. on Power Electronics*, vol. 12, no. 3, May 1997, pp.495-506.
- [6] X. Luo, Y. Liao, H. A. Toliyat, A. El-Antably, and T. A. Lipo, "Multiple couple circuit modeling of induction machines," *IEEE Trans. Ind. Appl.*, vol. 31, pp. 311–317, Mar./Apr. 1995.
- [7] H. R. Fudeh and C. M. Ong, "Modeling and analysis of induction machines containing space harmonics," *IEEE Trans. Power App. Syst.*, vol. PAS-102, pts. 1–3, pp. 2608–2628, Aug. 1983.
- [8] A. K. Wallace, R. Sp'ee, and H. K. Lauw, "Dynamic modeling of brushless doubly-fed machines," *Conf. Rec. IEEE-IAS Annu. Meeting*, San Diego CA, 1989, pp. 329–334.
- [9] A. K. Wallace and A. Wright, "Novel simulation of cage windings based on mesh circuit model," *IEEE Trans. Power App. Syst.*, vol. PAS-93, pp. 377–382, Jan./Feb. 1974.
- [10] A.R. Munoz, T.A. Lipo, "Complex Vector Model of the Squirrel-cage Induction Machine Including Instantaneous Rotor Bar Currents", *IEEE Trans. Ind. Appl.*, Vol. 35, No. 6, Nov/Dec 1999, pp. 1332-1340.
- [11] T. Dordea, *Masini electrice*, Ed II, editura Didactica si Pedagogica Bucuresti, 1977, pp.240.